JOURNAL OF VIROLOGY, Aug. 1996, p. 5106–5114 Vol. 70, No. 8
0022-538X/96/$04.00+0

Structural Analysis of Human Immunodeficiency Virus Type 1 Gag Protein Interactions, Using Cysteine-Specific Reagents

JASON MCDERMOTT, LORI FARRELL, ROBERT ROSS, AND ERIC BARKLIS*

Vollum Institute for Advanced Biomedical Research and Department of Molecular Microbiology and Immunology, Oregon Health Sciences University, Portland, Oregon 97201-3098

Received 13 February 1996/Accepted 29 April 1996

We have examined structural interactions of Gag proteins in human immunodeficiency virus type 1 (HIV-1) particles by utilizing cysteine mutagenesis and cysteine-specific modifying reagents. In immature protease-minus but otherwise wild-type (wt) particles, precursor $Pr55^{Gag}$ proteins did not form intermolecular cystines naturally but could be cross-linked at cysteines, and cross-linking appeared to occur across nucleocapsid (NC) domains. Capsid (CA) proteins in wt mature viruses possess cysteines near their carboxy termini at *gag* codons 330 and 350, but these residues are not involved in natural covalent intermolecular bonds, nor can they be intermolecularly cross-linked by using the membrane-permeable cross-linker bis-maleimido hexane. The cysteine at *gag* codon 350 (C-350) is highly reactive to thiol-specific modifying reagents, while the one at codon 330 (C-330) appears considerably less reactive, even in the presence of ionic detergent. These results suggest that the HIV-1 CA C terminus forms an unusually stable conformation. Mutagenesis of C-350 to a serine residue in the mutant C350S (C-350 changed to serine) virtually eliminated particle assembly, attesting to the importance of this region. We also examined a C330S mutant, as well as mutants in which cysteines were created midway through the capsid domain or in the C-terminal section of the major homology region. All such mutants appeared wt on the basis of biochemical assays but showed greatly reduced infectivities, indicative of a postassembly, postprocessing replicative block. Interestingly, capsid proteins of mature major homology region mutant particles could be cysteine cross-linked, implying either that these mutations permit cross-linking of the native C-terminal CA cysteines or that major homology regions on neighbor capsid proteins are in close proximity in mature virions.

The human immunodeficiency virus (HIV-1) Gag proteins are encoded by the viral *gag* gene and are synthesized as a polyprotein precursor, $Pr55^{Gag}$. Expression of $Pr55^{Gag}$ in eukaryotic cells is necessary and sufficient for the formation of virus-like particles (10, 14, 22, 34, 35). Immature particles are approximately 125 nm in diameter, are surrounded by a lipid bilayer, and show an electron-dense layer juxtaposed to the bilayer (35). In cells infected with wild-type (wt) HIV-1, the $Pr55^{Gag}$ precursor ordinarily is cleaved by the virally encoded protease (PR) to give an occasional processing intermediate (p41), and the mature viral Gag proteins, matrix (MA), capsid (CA), nucleocapsid (NC), and p6 (4, 19, 25, 29). Coincident with processing, HIV particles take on a new morphology: the particles become much more sensitive to disruption by nonionic detergents (36, 39), and they acquire an electron dense conical or cylindrical core (9).

Most of the knowledge acquired about Gag protein function has come from molecular genetic analysis of mutants. Mutations of MA are characterized by a reduction in membrane binding (33, 39), impaired assembly (8, 33) or assembly on intracellular membranes (8, 16), reduced incorporation of viral envelope products (Env) into virus particles (8, 43), and/or impaired Env function (39, 42). The capsid domain contains a region of Gag protein primary sequence homology shared among almost all primate and avian retroviruses, called the major homology region (MHR) (27, 37, 41). Mutations in the MHR can impair assembly (27) or can cause assembled particles to be noninfectious (27, 37). Several other mutations in CA block assembly (17, 38) or block virus infection at an undefined late stage of the virus life cycle (39). Mutations in NC also can cause a reduction in assembly. In addition, many NC mutations impair viral ability to encapsidate viral RNA (1, 11), supporting the notion that the Cys-His fingers in NC are required for specific encapsidation of viral RNA. Finally, mutations in p6 cause a reduction in virus budding under some conditions (12).

Although standard molecular genetic approaches have allowed identification of the functions of different Gag proteins, definition of subdomain interactions is in its infancy, and very little is known about how Gag proteins associate with each other to form a virus particle. To begin to identify important Gag-Gag protein contacts in virus particles, we have commenced a series of cysteine mutagenesis experiments aimed at assessing the importance of the Gag protein cysteine residues in the virus life cycle and at identifying important Gag protein associations by cysteine-specific cross-linking methods (18). Our studies have focused on $Pr55^{Gag}$ in immature virions and on the CA domain of mature virus particles, as it appears to make essential interprotein contacts in infectious virions (9). In this study, we have examined the status of wild-type (wt) HIV-1 Gag protein cysteines and of cysteines created in the HIV-1 capsid domain. Our results indicate that intermolecular cystine formation is not essential to particle assembly but that $Pr55^{Gag}$ proteins can be linked, apparently across their nucleocapsid cysteines. Biochemical and genetic analysis showed that the two HIV-1 CA cysteines at *gag* codons 330 and 350 did not form intramolecular cystines on the majority of capsid proteins and that mutagenesis of C-350 had profound effects on virus particle assembly. Additionally, creation of cysteines in the C-terminal portion of the HIV-1 MHR increased the efficiency of CA-CA cross-link formation and yielded virus particles that had wt characteristics but were poorly infectious. Taken to-

* Corresponding author. Phone: (503)-494-8098. Fax: (503)-494-6862.

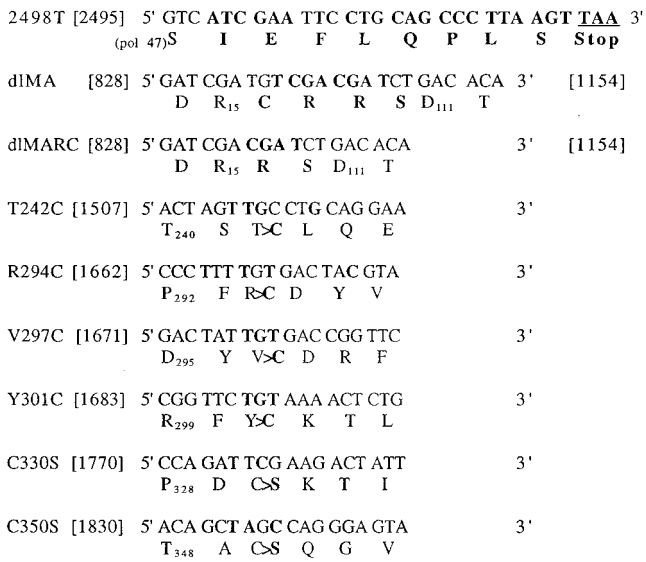

FIG. 1. HIV-1 Gag mutants. Mutant plasmids used are all HIVgpt vectors and were constructed by standard methods. The mutation in 2498T is an insertion which provides a premature stop codon to the *pol* gene and inactivates the protease protein. The mutations *dl*MA and *dl*MARC are both 316-nt deletions in the MA domain which remove 96 codons. In all cases, sequences are shown 5′ to 3′, altered or inserted nucleotides and residues are in boldface, nucleotide numbers for all 5′ and some 3′ nucleotides are in brackets, and codon numbers are subscripts.

gether, our results indicate that the C-terminal end of HIV-1 CA is extremely important to virus particle assembly and that MHR residues appear to mediate Gag protein associations, at least in the mature capsid domains.

MATERIALS AND METHODS

Recombinant plasmids. The parental wt plasmid used in this study is HIVgpt, which was derived from the HXBc2 HIV provirus (32). The plasmid has an active simian virus 40 origin of replication sequence which allows plasmid replication in transiently transfected COS7 cells (30). For infectivity assays using expression of the bacterial *gpt* gene as a selectable marker, the SV-A-MLVenv plasmid was used as previously described (30). Both the HIVgpt and the SV-A-MLVenv plasmids were generously provided by D. Littman (30). Mutant virus constructs (Fig. 1) were based on HIVgpt, and construction and sequencing followed standard protocols (28). One protease-minus (PR^-) version of HIVgpt, HIVgpt 2498T, was constructed by the insertion of an exogenous sequence that provides a stop codon at the N terminus of the *pol* gene product. The sequence from nucleotide (nt) 2495 is 5′ GTC ATC GAA TTC CTG CAG CCC TTA AGT TAA CTT AAG GGG GGA TCA GAT 3′; the underlined triplet provides a *gag* frame stop codon. HIVgpt *dl*MARC is a variation of HIVgpt *dl*MA, previously described (40). The notable difference is that the *dl*MARC construct does not introduce a cysteine: whereas the sequence of the *dl*MA construct, starting at nt 827 and ending at nt 1149, is 5′ AT CGA TGT CGA CGA TCT G 3′, the sequence of *dl*MARC is 5′ AT CGA CGA TCT G 3′. Note that the *dl*MARC PR^- construct is a combination of the dlMARC and 2498T.

Point mutants used in this study were as follows: T242C, in which the threonine at *gag* codon 242 was changed to a cysteine, giving the sequence 5′ ACT AGT **TGC** CT**G** CAG GAA 3′; R294C, in which the arginine at codon 294 was changed to a cysteine (5′ CCC TTT **TGT** GAC TA**C** GTA 3′); V297C, in which the valine at codon 297 was changed to a cysteine (5′ GAC TAT **TGT** GAC CGG 3′); Y301C, in which the tyrosine at codon 301 was changed to a cysteine (5′ CGG TTC **TGT** AAA ACT CTG CGC GCC GAG 3′); C330S, in which the cysteine at codon 330 was mutated to a serine (5′ CCA GAT **TCG** AAG ACT 3′); and C350S, with replacement of the cysteine at codon 350 with a serine (5′ ATG ACA GCT **AGC** CAG 3′). In all cases, mutated codons are underlined and altered nucleotides are in boldface. Note that in some but not all cases, additional conservative nucleotide changes were made to facilitate mutant screening by restriction digest analysis.

As a standard for Gag protein quantitation, we also expressed and purified a histidine-tagged capsid protein. To do so, the HIV-1 capsid coding region was cloned into plasmid pet15B. The resultant plasmid, pet15BHIV1147-1900, has a 5′ juncture sequence of 5′ G GAT CCC GCT G 3′ and a 3′ juncture sequence of 5′ AAT TCC TGC AGC CCG GGG GAT CC 3′. The expressed recombinant protein has non-CA N- and C-terminal amino acid additions of MGSSHHHH HHSSGLVPRGSHMLQDP and AQAMSQVTNSCPGDAANKARKQLAAA TAEQ(stop).

Cell culture, transfections, infections, and infectivity assays. COS7 and HiL cells ($CD4^+$ HeLa cells) were maintained in Dulbecco's modified Eagle's medium supplemented with 10% heat-inactivated fetal calf serum, penicillin, and streptomycin. COS7 cells were split from confluent plates 1:4 onto 10-cm-diameter plates 24 h before each transfection. Plasmid DNAs of HIVgpt wt or *gag* mutant HIVgpt constructs were transfected onto COS7 cells by calcium phosphate precipitation (13), and chloroquine (25 mM) was added to improve efficiency. For transfection of one plasmid, 14 μg of plasmid DNA was used, but for production of pseudotyped virus, 8 μg of SV-A-MLVenv plasmid was cotransfected with 8 μg of wt or mutant HIVgpt plasmid. Three days posttransfection, cell lysates and supernatants were collected as previously described (39). For infections, HiL cells on 10-cm-diameter plates were 10% confluent. Adsorption of virus was allowed to take place at 37°C in the presence of 4 μg of Polybrene per ml. Three days postinfection, plates were split 1:8 onto 10-cm-diameter plates containing selection medium (standard growth medium plus 50 μg of xanthine, 3 μg of hypoxanthine, 4 μg of thymidine, 10 μg of glycine, 150 μg of glutamine, and 25 μg of mycophenolic acid [GIBCO] per ml). Plates were refed with selection medium every 3 to 4 days until drug-resistant colonies formed. The number of colonies on each plate was used to calculate virus titers (gpt-resistant CFU per milliliter), and mutant infectivities were determined by comparison with wt HIVgpt titers derived in parallel experiments.

Hybridoma cells were grown in RPMI medium supplemented with 10% heat-inactivated fetal calf serum, penicillin, and streptomycin in tissue culture flasks. Antibody-containing medium was collected by centrifugation to remove cells and then frozen at −80°C, with 0.2% sodium azide added to aid in preservation.

Protein analysis. Medium supernatants of transfected COS7 cells were collected at 3 days posttransfection and filtered through a 0.45-μm-pore-size filter. The filtered supernatants were centrifuged at 4°C for 45 min at 274,000 × *g* (40,000 rpm in an SW41 rotor) through 2 ml of 20% sucrose in TSE (10 mM Tris hydrochloride, 100 mM NaCl, 1 mM EDTA, 0.1 mM phenylmethylsulfonyl fluoride [PMSF]). Pellets were resuspended in 100 μl of IPB (20 mM Tris hydrochloride [pH 7.5], 150 mM NaCl, 1 mM EDTA, 0.1% sodium dodecyl sulfate [SDS], 0.5% sodium deoxycholate, 1% Triton X-100, 0.02% sodium azide) plus 0.1 mM PMSF for electrophoresis or in TSE for other procedures. Cells from transfected plates were washed with 10 ml of ice-cold phosphate-buffered saline (PBS) twice and collected in 1 ml of PBS for each 10-cm-diameter plate. Cells then were gently pelleted and resuspended in 1 ml of IPB plus 0.1 mM PMSF and repelleted to remove debris. Supernatant and cell samples were prepared for electrophoresis by addition of an equal volume of 2× sample buffer (12.5 mM Tris hydrochloride [pH 6.8], 2% SDS, 20% glycerol, 0.25% bromophenol blue) plus β-mercaptoethanol (B-Me) to 5% followed by boiling for 4 to 5 min (16). Samples were subjected to SDS-polyacrylamide gel electrophoresis (PAGE (24)) and electroblotted onto a nitrocellulose filter, and Gag proteins on filters were immunodetected by using procedures previously described (21). Two primary antibodies were used for the detection of p24: Hy5001, a mouse anti-p24 monoclonal antibody (the kind gift of Epitope Inc., Beaverton, Oreg.), used at 1:20,000 dilution; and Hy183, a mouse hybridoma monoclonal antibody (clone H12-5C; obtained through the AIDS Research and Reference Reagent Program, Division of AIDS, National Institute of Allergy and Infectious Diseases, from Bruce Chesebro, used at 1:30 dilution from medium of cells grown in culture. The primary antibody used for the detection of MA was Hy3H6.D4P (the kind gift of Epitope Inc.). In all cases, the secondary antibody used was a goat anti-mouse immunoglobulin G-alkaline phosphatase conjugate (Promega). Immunodetected bands on filters were quantitated either by scanning densitometry with a Bio-Rad model 620 video densitometer on reflectance mode (39) or by obtaining a computer image file of the filter with a Hewlett-Packard color flatbed scanner and processing the image with the NIH Image software package. Efficiency of proteolytic processing was calculated by dividing the density units of individual proteolytic product bands of each sample by the total Gag density of that sample.

Sucrose density gradient fractionation of virus particles was performed as described (39, 40, 44). Briefly, extracellular virions were isolated by pelleting medium supernatant from transfected COS7 cells through a 4-ml, 20% sucrose cushion in TSE. The pellets were resuspended in TSE and applied to sucrose gradients consisting of 1.1-ml layers of 20, 30, 40, and 50% sucrose in TSE which had been allowed to mix by sitting for 1 h. Gradients were centrifuged at 300,000 × *g* (50,000 rpm on an SW50.1 rotor) overnight at 4°C, and 400-μl fractions were collected from top to bottom. Fractions were analyzed for sucrose density and Gag protein levels by densitometric quantitation of immunodetected bands. Gag protein levels were normalized to the band with highest Gag protein level from each gradient.

Cross-linking and chemical reactivity methods. Iodine cross-linking of cysteine residues was performed as described previously (16, 31). For cross-linking with bis-maleimido hexane (BMH; Pierce) treatments, virus particles or proteins were prepared as described above and resuspended in 200 μl of TSE or PBS. BMH was prepared fresh as a 100 mM solution in dimethyl sulfoxide (DMSO), and viral samples were split into equivalent 100-μl fractions, treated with BMH (1 μl of 100 mM BMH in DMSO) or mock treated (1 μl of DMSO), vortexed

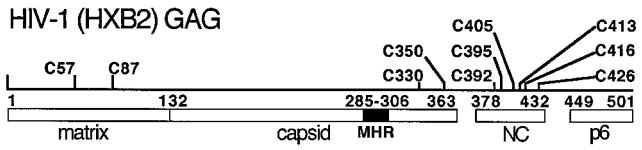

FIG. 2. Locations of cysteine residues in HIV Pr55^{Gag}. The HIV-1 (HXBc2) Pr55^{Gag} protein consists of four domains, matrix (MA), capsid (CA), nucleocapsid (NC), and p6, that are cleaved to maturation by the virally encoded protease (PR) during the budding process. The precursor polypeptide is 501 codons in length, and the juncture codons are indicated (note that both the CA/NC and NC/p6 junctures are formed by the excision of small peptides of unknown function, p1 and p2). Pr55^{Gag} contains 10 cysteines, which are indicated on the top bar with codon numbers. The HIV MHR is indicated and spans *gag* codons 285 to 306.

gently, and incubated at room temperature for 1 h. Reactions were terminated by the addition of 2× sample buffer plus β-Me to 5%, and the samples were boiled for 3 to 5 min (18). For detergent treatment experiments, Triton X-100 or lithium dodecyl sulfate (LDS) was used at a final concentration of 0.25% in cross-linking reactions.

Biotin-maleimide (Sigma) reactions were carried out on proteins prepared as described above and resuspended in TSE. Biotin-maleimide was prepared as a 100 mM solution in DMSO and then diluted to 10 mM in 10 mM Tris hydrochloride (pH 7.4). Reactions were performed in a 100-μl total volume with the addition of 10 μl of 10 mM biotin-maleimide prepared as described above or 10 μl of 10% DMSO in 10 mM Tris hydrochloride (pH 7.4) for the mock treatment. Triton X-100 and LDS were used at 0.25% (final concentration) in specified reactions. Reactions were allowed to proceed in the dark on ice for 1 h and were terminated by the addition of 2× sample buffer plus β-Me to 5%. Biotinylated proteins were identified by mobility shift and with alkaline phosphatase-conjugated streptavidin on electroblotted filters.

Chemical cleavage of proteins. Specific protein cleavage at cysteine residues by 2-nitro-5-thiocyanobenzoic acid (NTCB; Sigma) was done as previously described (2), with modifications. NTCB was prepared fresh as a 2.24-mg/ml solution (1 M) in buffer bob (6 M guanidine hydrochloride, 200 mM Tris hydrochloride [pH 8.0], 0.1 mM EDTA [pH 8.0], 0.1 mM dithiothreitol [DTT]). Cleavage reaction mixtures were prepared by mixing 175 μl of buffer bob with 25 μl of protein sample (in TSE), and reactions were initiated by addition of 50 μl of NTCB solution and vortexing. Cleavage reactions took place at 37°C in the dark on a rocking platform for 20 to 75 h. Reactions were terminated by the addition of β-Me to 1%, after which samples were dialyzed two times for 2 h each in a fume hood against 1 liter of 50 mM ammonium bicarbonate (pH 8.0). Dialyzed samples were vacuum dried overnight, resuspended in 150 μl of IPB–150 μl of 2× sample buffer–1.5 μl β-Me, and subjected to SDS-PAGE and immunoblotting. For successive biotin-maleimide and then NTCB treatments, samples were processed according to the procedure for biotin-maleimide modification except that the reaction mixtures were incubated at room temperature 2 h and no β-Me was added to terminate the reaction. Prior to NTCB cleavage, 10-μl aliquots were set aside for electrophoresis, while the remainder of the biotin-maleimide reaction mixtures were combined with 1.5 ml of buffer bob plus 300 μM DTT, after which 400 μl of 10 mM NTCB (in buffer bob plus 300 μM DTT) was added. Cleavage reactions then proceeded as described above.

RNase protection and reverse transcriptase reactions. RNase protection assays using the HIV 831-680 riboprobe were performed as previously described (40, 44). The riboprobe spans the HIV major splice donor sequence and thus will detect both spliced and unspliced transcripts. Exogenous reverse transcriptase assays were performed as previously described (39), and results were normalized to densitometrically determined Gag levels from immunoblots. To assay reverse transcriptase activities on native templates, endogenous reverse transcriptase reactions were performed on permeabilized pelleted particles, using previously established reaction incubations. Total nucleic acid was isolated from each reaction mix, and minus-strand strong-stop DNA was assayed by RNase protection using a 151-nt sense strand probe.

RESULTS

Cysteine-specific cross-linking of wt HIV-1 Gag proteins. There are a total of 10 cysteines encoded by the HIV-1 *gag* gene (Fig. 2), two in the matrix domain (MA), two in the capsid domain (CA), six in the nucleocapsid domain (NC), and none in p6. The NC cysteines are absolutely conserved among over 70 different HIV-1 *gag* genes that have been sequenced (26), and the two MA cysteines are conserved to a very high degree; one cysteine is invariant, while the other cysteine is absent in only three isolates (26). The two CA cysteines also are well conserved. The first cysteine (*gag* codon 330) is absolutely conserved, and the second cysteine (C-350) is conserved in all but one isolate (26). The corresponding CA cysteine residues are present and conserved in HIV-2 ROD and SIV isolates (20), but these viruses encode an additional cysteine in the central portion of their capsid domains. Of these cysteine residues, evidence indicates that NC cysteines form two zinc fingers important in viral RNA encapsidation (1). Additionally, MA cysteines have been located in nuclear magnetic resonance and X-ray structures of the matrix domain. However, it is unclear how CA cysteines contribute to HIV function and how MA, CA, and NC cysteines interact in Pr55^{Gag}. These studies were performed to clarify the roles of the HIV-1 CA cysteines (C-330 and C-350) in the viral life cycle and to combine cysteine mutagenesis with cross-linking and chemical reactivity protocols to probe virus particle structure (18).

To determine whether HIV-1 Gag cysteines are in close proximity to cysteines on neighboring Gag proteins, we initially ran proteins from immature and mature virus particles on nonreducing gels and found no evidence for intermolecular Gag protein cystine formation (23). As a second step, we used membrane-permeable BMH to cross-link cysteines in intact mature and immature PR$^-$ virus particles. When wt mature HIV particles were subjected to BMH cross-linking and the protein products were immunodetected with either anti-CA or anti-MA antibodies, no novel cross-linked species were identified (Fig. 3, lanes A, B, E, and F). These data imply either that BMH cannot penetrate mature virions or that cysteines on mature MA or CA proteins were not in close enough proximity to cysteines on neighboring proteins to cross-link. In contrast, when immature PR$^-$ particles were subjected to BMH cross-linking, a novel protein band at 110 kDa was detected with both the CA (lane D) and MA (lane H) antibodies, along with an additional, less pronounced band of unknown origin at about 100 kDa. This result is consistent with the supposition that at least one pair of cysteine residues on neighboring Pr55^{Gag} molecules can be cross-linked and is similar to our previous findings with Moloney murine leukemia virus PrGag

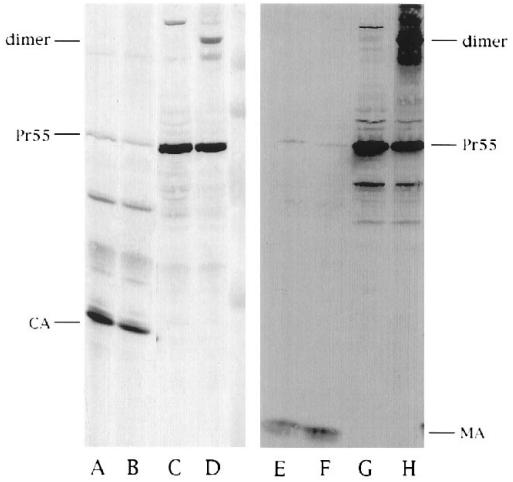

FIG. 3. Cross-linking of HIV-1 Gag proteins. wt (lanes A, B, E, and F) or PR$^-$ (lanes C, D, G, and H) HIVgpt particles were mock treated (lanes A, C, E, and G) or treated with BMH (lanes B, D, F, and H) to cross-link neighboring cysteine residues. Samples were separated by SDS-PAGE and electroblotted, and Gag proteins were detected by immunoblotting with either the anti-CA antibody (lanes A to D) or the anti-MA antibody (lanes E to H). HIV Gag proteins MA, CA, and Pr55^{Gag} are indicated, as are putative 110-kDa Pr55^{Gag} dimers. Also evident are PrGag-Pol proteins (lanes C and G) and 100-kDa species (lanes D and H).

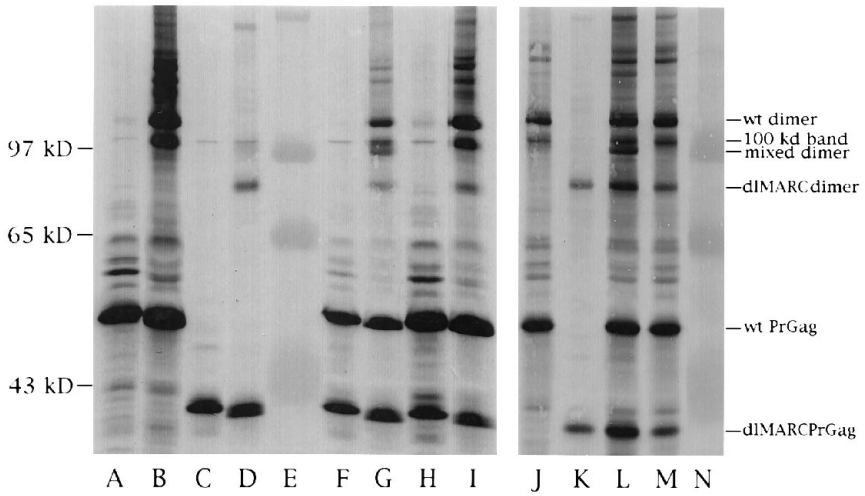

FIG. 4. Composition of cross-linked Gag species. Gag proteins from virus particles that were mock treated (lanes A, C, F, and H) or BMH treated (lanes B, D, G, I, J, K, L, M, and N) were electrophoresed and immunodetected with an anti-CA antibody as described for Fig. 2. Virus particles derived from COS7 cells transfected with PR$^-$ (lanes A, B, and J), *dl*MARC PR$^-$ constructs, (lanes C, D, and K), particles from cells cotransfected with PR$^-$ and *dl*MARC PR$^-$ constructs, (lanes F, G, and L), and particles mixed from cells singly transfected with PR$^-$ and *dl*MARC PR$^-$ constructs (lanes H, I, and M). Standard molecular weight sizes are indicated on the left and derive from marker lanes E and N. wt and *dl*MARC PrGag proteins, homodimers, mixed dimers, and the 100-kDa band of unknown origin are indicated on the right.

protein cross-linking (18). Note also that the most slowly migrating PrGag-Pol band in lane C disappears upon cross-linking (lane D), presumably because PrGag-Pol proteins cross-link to generate a species which does not enter our running gels readily.

The appearance of a 110-kDa band upon cross-linking of immature virus particles was consistent with the presence of a Pr55^{Gag} dimer but could also be due to the cross-linking of Pr55^{Gag} to an unknown protein of approximately 55 kDa. To analyze the composition of the putative dimers, we constructed a matrix deletion Pr55^{Gag} protein, *dl*MARC PR$^-$, which retains N- and C-terminal MA sequences but is deleted from codons 15 to 111. The *dl*MARC mutant is similar to the previously described *dl*MA mutant (40), which assembles conditionally infectious virus particles, except that *dl*MARC is two residues shorter and retains no cysteines in the MA domain. To examine the composition of Gag-reactive cross-linked molecules, we subjected PR$^-$ wt and *dl*MARC proteins in virus particles to BMH treatments (Fig. 4). Again, BMH treatment of PR$^-$ particles yielded a new band at 110 kDa and a less pronounced 100-kDa band of unknown origin (lane B). Cross-linking of *dl*MARC PR$^-$ virus particles produced an additional band at approximately 82 kDa, consistent with the predicted size of a *dl*MARC cross-linked dimer (lane D). When separately isolated PR$^-$ and *dl*MARC PR$^-$ particles were mixed prior to cross-linking, the predicted homodimer bands of 82 and 110 kDa were observed, as was the 100-kDa band of unknown origin (lane I). In contrast to the mixing experiment, when PR$^-$ and *dl*MARC PR$^-$ constructs were cotransfected, cross-linking of the isolated virus particles showed an additional band at approximately 96 kDa (lane G). This new band corresponds to the expected size for a mixed dimer of PR$^-$ and *dl*MARC PR$^-$ Gag proteins. However, since the mixed dimer 96-kDa band migrated so closely to the unknown 100-kDa band, we repeated the cross-linking experiment and ran all cross-linked products side by side (Fig. 4, lanes J to M). Again the wt dimer (lane J) and *dl*MARC (lane K) dimers were observed, and the mixed particles showed homodimers only (lane M). However, in addition to the homodimers, the co-transfection experiment (lane L) showed a heterodimer at 96 kDa. We conclude from these experiments that BMH cross-links neighboring Gag proteins at cysteine residues. Furthermore, neither mature MA nor CA cross-links (Fig. 3), and PrGag does not require MA cysteines to cross-link (Fig. 4). Independent experiments showed that a PrGag protein deleted for all of the cysteine residues in the NC domain was impaired in cross-linking (data not shown). While we cannot exclude arguments that NC mutant proteins fold differently from wt PrGag proteins, our results are consistent with the interpretation that cross-linking of HIV-1 Pr55^{Gag} occurred via the cysteines in the NC domain. This result is similar to what we have observed with M-MuLV PrGag proteins (18) and suggests that NC in Gag precursors may play an important role in multimerization of Gag proteins (3, 7).

Analysis of HIV-1 capsid protein cysteines. Since HIV-1 capsid protein cysteines are well conserved (26) and in close proximity in the primary sequence (only 20 residues apart), we were interested in examining the status of these two residues. Consequently, cysteines at *gag* codons 330 and 350 were mutated separately to encode serines in the mutants C330S and C350S (Fig. 1). When wt, C330S, and C350S HIVgpt constructs were transfected into COS7 cells, the standard Pr55, p41, and CA proteins were detected in lysates of wt (Fig. 5, lane A)- and C330S (lane C)-transfected cells. However, we consistently detected no capsid-related proteins in lysates from cells transfected with the C350S mutant (lanes B and D) when anti-CA antibody Hy5001 was used. The absence of C350S proteins in cell lysates could be due to something as trivial as failed transfections, and so a parallel immunoblot was performed with the second anti-CA monoclonal antibody, Hy183. As illustrated (lanes E to H), the second monoclonal antibody readily detected wt (lane E), C330S (lane G), and C350S (lanes F and H) Pr55, p41, and CA proteins in transfected cell lysates; these results suggest that the C350S mutation altered the Hy5001 epitope so that the mutant protein was no longer recognizable by this antibody on immunoblots. Using the Hy183 monoclonal antibody, which recognizes wt, C330S, and C350S proteins, we examined particle-associated Gag protein

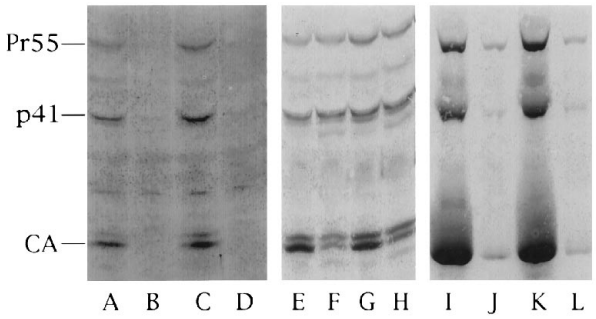

FIG. 5. Expression, release, and antibody reactivity of mutant Gag proteins. Cell lysates (lanes A to H) and virus particles from medium supernatants (lanes I to L) were collected from cells transfected with wt (lanes A, E, and I), C330S (lanes C, G, and K), and C350S (lanes B, D, F, H, J, and L) HIVgpt constructs as described in Materials and Methods. Samples were subjected to SDS-PAGE and electroblotted, and Gag proteins were immunodetected with anti-CA antibody Hy5001 (lanes A to D) or Hy183 (lanes E to L). Pr55, p41, and CA proteins are as indicated.

levels in medium supernatants of transfected cells as a measure of the efficiency of wt and mutant proteins in directing the assembly and release of virus particles. As shown in lanes I and K, wt and C330S proteins were released efficiently from transfected cells. In contrast, the total amount of Gag protein released from C350S-transfected cells was 10- to 30-fold lower than that seen for its counterparts. These results indicate that the C350S mutation has a drastic effect on HIV particle assembly. At least two mechanisms might account for the C350S assembly defect: the mutation might cause a mislocalization of the protein within cells, or it could interfere with interactions that are necessary for particle assembly. Because results from subfractionation and immunofluorescence studies appeared indistinguishable for the wt and C350S proteins (data not shown), we believe that the C350S mutation interferes with assembly by disrupting Gag protein contacts with either membranes, viral RNA, or other proteins.

The fact that the C330S mutant assembled virus particles whereas the C350S mutant was assembly defective seems to discount the notion that these two residues form an intramolecular cystine. Furthermore, nonreducing gels showed little if any evidence for intermolecular cystine bridge formation between capsid proteins or $Pr55^{Gag}$ proteins (23). However, we were interested in directly testing the accessibility of the capsid cysteines. To do so, wt HIVgpt virus particles were treated with biotin-maleimide, which can biotinylate free thiols. Treatments were performed in the absence of detergent, in the presence of Triton X-100 (which dissembles mature but not immature HIV particles [39]), or in the presence of LDS (which dissembles both mature and immature HIV particles). Since biotin-maleimide is not membrane permeable in the absence of detergents, it is not surprising that the immunoblot profile of biotin-maleimide-treated samples was comparable to that of the mock-treated culture (Fig. 6; compare lanes B and E with lane A and lanes I and L with lane H). When biotin-maleimide reactions occurred in the presence of either detergent, one slightly lower mobility CA band (biotin-CA) was observed, and 30 to 70% of the capsid protein was shifted to this mobility when Hy183 was used for detection (lanes J, K, M, and N). However, when Hy5001 was used as a detection reagent, there was an apparent reduction in the amount of CA, and no biotin-CA was observed (lanes C, D, F, and G). We interpret these results to indicate that the biotin-CA band consists of CA biotinylated at C-350, CA biotinylated at C-350 plus C-330, or a combination of the mono- and dibiotinylated species.

In contrast to biotinylation results in the presence of Triton X-100 or in the absence of detergent, when particles were treated with LDS, there was evidence of lower mobility of Pr55 and p41 species as detected by Hy183 (lanes J and M). This result is consistent with previous observations that immature HIV particles are resistant to dissembly by nonionic detergents (16, 36) but also suggests that none of the HIV-1 PrGag cysteine residues were accessible to biotin-maleimide unless immature particles were completely disrupted. Additionally, since neither p41, Pr55, nor their biotinylated counterparts were visible when biotin-maleimide-, LDS-treated proteins were probed with Hy5001, it would appear that all biotinylated and biotin-Pr55 species were modified at C-350.

To extend our observations, wt Gag proteins were mock or biotin-maleimide treated and then subjected to NTCB cleavage at free cysteines. In this case, biotinylated cysteines should

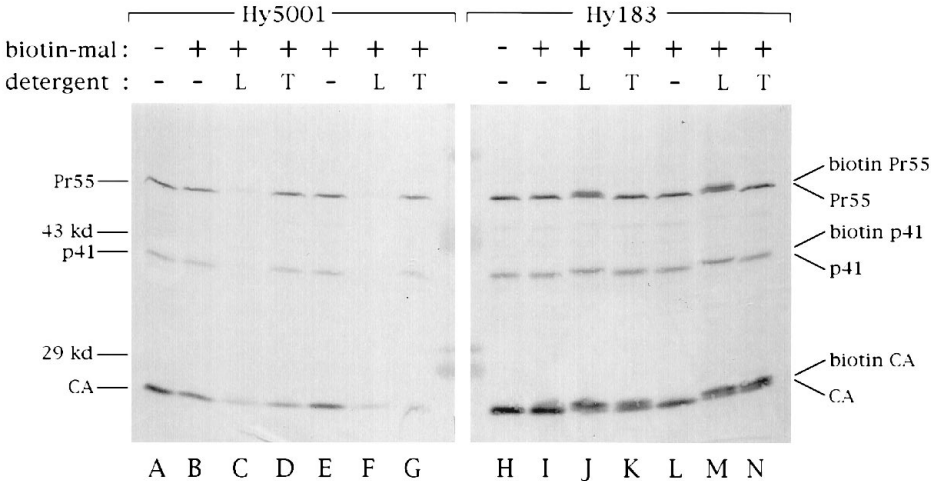

FIG. 6. Biotin-maleimide reactivity of HIV-1 capsid proteins. wt HIVgpt virus particles were mock treated (−; lanes A and H) or biotin-maleimide treated (+; lanes B to G and I to N) in the absence of detergent (−; lanes B, E, I, and L) or in the presence of 0.25% Triton X-100 (T; lanes D, G, K, and N) or 0.25% LDS (L; lanes C, F, J, and M). After treatments, proteins in samples were separated by SDS-PAGE, electroblotted, and immunodetected with anti-CA antibody Hy5001 (lanes A to G) or Hy183 (lanes H to N). Note that Hy5001 does not recognize C350S mutant Gag proteins, while Hy183 does (see Fig. 5). Marker protein sizes, Gag proteins Pr55, p41, and CA, and biotinylated species are as indicated.

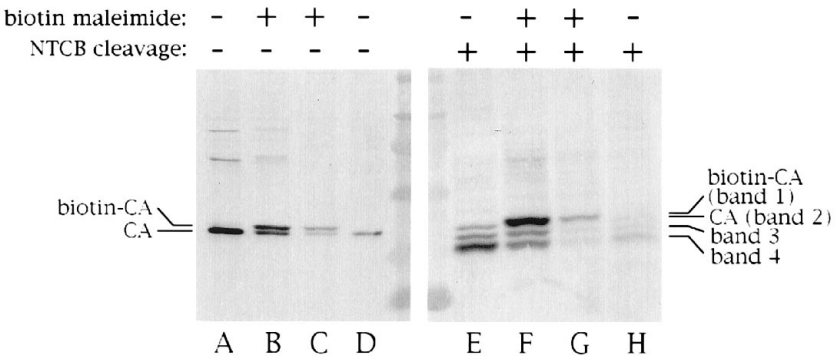

FIG. 7. Cleavage of HIV-1 capsid proteins at cysteine residues. wt (lanes A, B, E, and F) or *dl*MARC (lanes C, D, G, and H) HIVgpt particles were mock treated (lanes A, D, E, and H) or treated with biotin-maleimide (lanes B, C, F, and G), after which proteins were processed for electrophoresis (lanes A to D) or NTCB cleaved at nonbiotinylated cysteines and processed for electrophoresis. Electrophoretically separated proteins were electroblotted and immunodetected with anti-CA antibody Hy183. Four different capsid-derived proteins are indicated: band 1 (biotin-CA), band 2 (CA), band 3, and band 4.

be resistant to NTCB cleavage, and cleavage should occur only at residues that were unable to be biotinylated. In this experiment, we used two different HIVgpt preparations, wt and *dl*MARC, both of which form mature virus particles that appear identical with respect to their capsid proteins. As expected, completely untreated samples yielded only one capsid band (Fig. 7, lanes A and D), while biotin-maleimide-reacted samples (which had not been NTCB cleaved) gave the additional lower-mobility band seen in Fig. 6 (lanes B and C). When unbiotinylated proteins corresponding to lanes A and D were cleaved with NTCB, several bands were seen (lanes E and H), one presumably corresponding to CA which was not cleaved by NTCB (band 2) and others of higher mobility (bands 3 and 4), cleaved at C-330 and/or C-350 with NTCB. When samples were first reacted with biotin-maleimide and then cleaved by NTCB, the relative amounts of material in bands 1 (biotin-CA) and 2 (CA) increased (lanes F and G), consistent with the notion that biotin-maleimide reactions protected CA from NTCB cleavage. Interestingly, the amount of material in band 3 remained constant regardless of whether the samples received biotin-maleimide pretreatment. In contrast, biotin-maleimide pretreatment caused a clear decrease in the relative amount of band 4 (compare band 4 in lanes F and E and in lanes G and H). Since C-350 preferentially reacts with biotin-maleimide (Fig. 6), this result suggests that band 4 is the cleavage product at C-350 and band 3 is the cleavage product at C-330. This result is paradoxical since the C-330 cleavage product (band 3) should be smaller than the C-350 cleavage product (band 4). However, this type of gel migration anomaly has been observed in cases in which the C termini of avian retrovirus proteins are naturally cleaved or artificially truncated (6, 7). Our results indicate that C-350 is highly reactive to biotin maleimide but that C-330 appears considerably less reactive. The lack of C-330 reactivity could be due to its inaccessibility, even in the presence of ionic detergent. Alternatively, the thiol at C-330 could be blocked by an as yet undetermined low-molecular-weight factor. However, if this is the case, the factor could not be necessary for virus assembly, since the mutant C330S does assemble virus particles.

Phenotypes of HIV-1 cysteine substitution mutants. Since we examined the status of the two natural cysteines in the HIV-1 capsid proteins, we thought that it might be useful to examine what occurred when additional cysteines were introduced into the capsid coding region. In addition to the C330S and C350S mutants (Fig. 1), we chose to look at four others. One mutant, T242C (Fig. 1), is at a site where a linker insertion mutation killed virus infectivity and impaired proteolytic processing of the $Pr55^{Gag}$ precursor (39). In addition, three mutations, R294C, V297C, and Y301C, were created in the C-terminal portion of the capsid domain MHR (Fig. 1). Previously, others found that mutations in the most conserved, amino-terminal residues of the MHR killed virus infectivity and could block assembly (27, 37). We chose residues 294, 297, and 301 since nuclear magnetic resonance studies suggested that the HIV MHR forms an amphiphatic helix in solution with R-294 on the hydrophilic face and V-297 and Y-301 on the hydrophobic face (5). We felt that it was possible to determine whether cysteines introduced at these positions might interfere with assembly or, if not, might be used to probe structural features of the MHR.

For analysis, mutant and wt HIVgpt constructs first were transfected into COS7 cells, and virus particle release levels were assayed as described for Fig. 5. Similar to the C330S mutant and in contrast to the C350S mutant, medium levels of T242C, R294C, V297C, and Y301C were all roughly comparable to wt levels (data not shown), suggesting that these mutants were not defective for virus assembly. Furthermore, all well-released mutants made particles of wt density and were appropriately processed (data not shown).

Since particles released by T242C, R294C, V297C, Y301C, or C330S were not grossly defective, we tested the abilities of Gag mutant virions to infect target cells. To do so, wt or mutant HIVgpt constructs were cotransfected with an envelope expression construct into COS7 cells, and filtered medium supernatants were collected. For infectivity assays, infectious events were monitored by transduction of the proviral *gpt* gene. Thus, particles were applied to target HiL cells, which subsequently were split into *gpt* selective medium and grown until the appearance of drug-resistant colonies. In all cases, mutant and wt HIVgpt infections were performed in parallel. Titers, in CFU per milliliter, were calculated on the basis of colony numbers, and mutant titers were compared with wt titers obtained in infections performed at the same time (Table 1). Interestingly, the infectivities of all of the capsid domain single-substitution mutants were considerably lower than that of wt. The near-zero titers for the C350S mutant were expected, given its defect in release. However, of the other mutants, only T242C showed appreciable titers, 5 to 20% that of wt. In contrast, C330S titers were 1 to 5% of wt titers, and all mutations in the MHR (R294C, V297C, and Y301C) gave titers less than 1% of wt titers.

Why are the infectivities of the capsid domain single-substi-

TABLE 1. Infectivities of HIV *gag* mutants[a]

Construct	Titer (CFU/ml)	HIVgpt wt titer (CFU/ml)	% Infectivity
HIVgpt	2,296	2,296	100
T242C	416	2,178	19.1
	34	874	3.9
	102	749	13.6
	192	2,007	9.6
R294C	20	7,847	0.3
	5	1,504	0.3
	7	3,831	0.2
V297C	5	2,451	0.2
	13	3,831	0.3
	21	1,504	1.4
	4	2,007	0.2
Y301C	17	2,451	0.7
	12	2,451	0.5
	22	7,831	0.3
	0	1,504	0
	3	3,831	0.1
C330S	61	1,400	4.3
	41	2,451	1.7
C350S	0	1,400	0
	1	2,451	0.04

[a] Each HIVgpt-based construct was cotransfected with SV-A-MLVenv into COS7 cells, and 3 days later, cell supernatants were used to infect HiL cells. Infections and selections for mycophenolic acid-resistant colonies were performed as described in Materials and Methods. The value for the HIVgpt wt titer was calculated as an average of 11 independent infectivity experiments. Replicate experiments were performed with different DNA plasmid preparations, at different times, or both. Infectivities for each mutant were determined by the ratio of its titer versus the HIVgpt wt titer in a parallel experiment.

tution mutants so low? RNase protection assays showed that the T242C, R294C, V297C, Y301C, and C330S mutant particles packaged roughly wt levels of genomic viral (data not shown), and so the mutants do not appear defective for RNA encapsidation. Similarly, efficiently released mutant particles possessed wt levels of exogenous template reverse transcriptase activity (39) and endogenous reverse transcriptase minus-strand strong-stop product levels (data not shown), suggesting that the initial steps of reverse transcription are not impaired. Thus, it seems that our capsid mutants are defective either for virus entry into target cells or at an as yet undefined postentry step of infection. These results are reminiscent of those observed for some other HIV capsid mutants (39).

Cross-link analysis of cysteine substitution mutants. To probe the cysteines introduced in the capsid domain, particles were isolated from medium supernatants of transfected COS7 cells and either mock treated or cross-linked at cysteine residues with BMH (Fig. 8). As expected (Fig. 3), mature wt particles showed little evidence of capsid protein cross-linking (Fig. 8, lane B) compared with the mock treatment (lane A). Similar results were obtained with T242C (lanes C and D). In contrast, BMH treatment of C330S and MHR mutant particles resulted in the appearance of anti-CA-reactive bands at 46-50 kDa, consistent with CA-CA dimers. The 46- to 50-kDa products show slightly different mobilities which vary by mutant. These variations may be due to mobility differences of dimers depending on the exact location of the cross-link. However, an alternative hypothesis, that CA monomers cross-link to unknown 22- to 26-kDa proteins, cannot be ruled out.

Given the lack of putative CA-CA dimers for wt HIVgpt, it was surprising that the C330S mutant showed a putative dimer band (Fig. 8, lane L). One explanation for this result is that the C330S mutation alters the conformation of CA in virus particles, such that C350 is placed in close proximity to C350 in neighbor molecules and is able to form a cross-link. An alternative explanation for this observation is that in wt particles, C-330 and C-350 preferentially form an intramolecular cross-link, and the absence of a suitable intramolecular partner in the C330S mutant leaves C-350 free to form intermolecular cross-links. While this interpretation might imply that cross-linking to form dimers always will occur when there is an odd number of cysteines in CA, the lack of cross-linking for T242C, which has three cysteines, argues against this implication.

As indicated above, all three MHR cysteine substitution mutants showed putative CA-CA dimer species (Fig. 8, lanes F, H, and J). These cross-linked species disappeared when virus particles were treated with either 0.1% Triton-X 100 or 0.1% SDS (data not shown), indicating that the mature virus particle structure was necessary for cross-link species to appear. Our results with R294C, V297C, and Y301C are consistent with the notion that MHR domains are close enough to be cross-linked in neighboring molecules, possibly forming an interface between capsid domains in mature particles. However, one caveat is that MHR cysteine mutations might cause a conformational change such that another CA cysteine (C-330 or C-350) is able to cross-link or that mixed cross-links might form. If this is the case, the conformational change appears to require cysteine substitutions at specific locations, since T242C did not cause the appearance of a significant cross-link band.

DISCUSSION

There are 10 cysteines in the HIV-1 Gag protein: two in the matrix domain, two at the C terminus of the capsid domain, and six involved in the two zinc finger motifs in NC (Fig. 2). Since we have not found evidence for PrGag or CA dimers in nonreducing gels, it does not appear that intermolecular cystine formation is essential to particle formation. However, PrGag proteins can be cross-linked at cysteines with BMH to form dimers, and cross-linking appears to occur in the NC domain (Fig. 3 and 4). In contrast to PrGag, we found no evidence for cross-linking of CA domains in mature wt particles (Fig. 4 and 8). One trivial explanation for this observation might be that the HIV-1 CA domain cysteines (C-330 and C-350) naturally form an intramolecular cystine. However, our

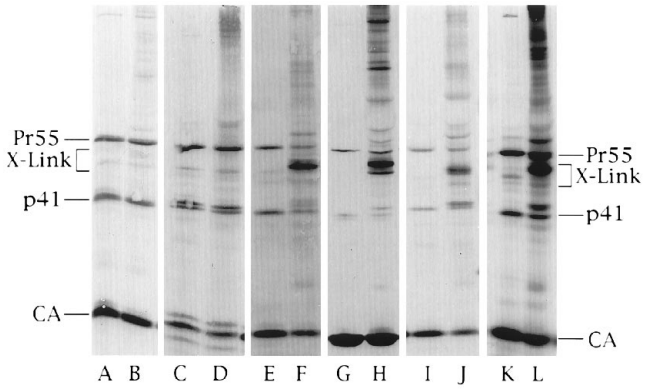

FIG. 8. Chemical cross-linking of HIV mutants. wt (lanes A and B) and mutant T242C (lanes C and D), R294C (lanes E and F), V297C (lanes G and H), Y301C (lanes I and J), and C330S (lanes K and L) HIVgpt particles were mock treated (lanes A, C, E, G, I, and K) or treated with BMH (lanes B, D, F, H, J, and L) to cross-link neighboring cysteine residues. Samples were subjected to SDS-PAGE and electroblotted, and Gag proteins were immunodetected with anti-CA antibody Hy183. HIV Gag proteins Pr55, p41, and CA are indicated, as are putative CA homodimer bands.

ability to biotinylate C-350 with biotin-maleimide (Fig. 6) argues against the existence of a natural intramolecular C-330–C-350 disulfide on the majority of capsid proteins. Interestingly, C-330 appears resistant to biotinylation, even in the presence of ionic detergent (Fig. 6 and 7). This observation suggests that the C-330 thiol could be chemically blocked. However, an alternate explanation is that the CA C terminus forms a secondary structure that is stable to ionic detergent. Indeed, the anomalous gel migration of cysteine cleavage products (Fig. 7) suggests that this is the case and is reminiscent of results with C-terminally modified avian retrovirus capsid proteins (6, 7). Although we currently have no direct evidence, we also would predict that the C-terminal cysteines of HIV-2 and simian immunodeficiency virus will possess the same chemical reactivities as those of HIV-1 CA. In this regard, it is noteworthy that HIV-2 and simian immunodeficiency virus encode CA cysteines besides those near the C terminus. On the basis of their nonconservation, it seems likely that these additional cysteines may interact with virus accessory proteins, such as Vpx, which are not present in HIV-1.

In our molecular genetic analyses, we found that the C330S mutation gave a phenotype that is similar to that of many other retrovirus capsid domain mutants. The infectivity of the C330S mutant was much less than that of wt (Table 1), but there was no apparent reduction in particle assembly (Fig. 3). Also, there were no apparent alterations in virus structure, as judged from proteolytic processing, sucrose gradient profiles, RNA levels, or reverse transcriptase activities (data not shown), although thorough electron microscopy studies were not done. These results suggest that the C330S mutation impairs either virus entry or postpenetration processes. In contrast to C330S, mutant C350S showed the most drastic effect on HIV assembly that we have observed for a single-residue substitution (Fig. 5). This might seem surprising for a conservative mutation of a cysteine which does not appear to be involved in consistent intra- or intermolecular cystine formation and could be due either to alteration of important interprotein assembly contacts or to mislocalization of the mutant Gag proteins. In this regard, we have found that the C350S immunofluorescence pattern appeared like that of wt, as did the membrane-versus-cytosol fractionation pattern (data not shown), suggesting that the mutation does not affect subcellular localization. Consequently, our hypothesis is that the C350S mutation changes an important CA C-terminal conformation that is a prerequisite for Gag protein oligomerization and particle assembly.

Insofar as CA cysteine substitution mutations are concerned, three were created in the C-terminal portion of HIV-1 MHR, since this region has been modeled to form an amphipathic helix (5), and one mutation was created at HIV *gag* codon 242, near a site which, when mutated by linker insertion, had a slight effect on assembly and processing (39). All of these mutants had phenotypes similar to that of the C330S mutant, although T242C was three times more infectious than C330S, and the MHR mutants were considerably less infectious (Table 1). When T242C, R294C, V297C, Y301C, and C330S were subjected to BMH cross-linking, T242C capsid proteins showed little evidence of cross-linking, while the other mutants gave putative CA-CA dimer bands (Fig. 8). The results with C330S were surprising given that wt CA proteins did not cross-link (Fig. 3 and 8). One explanation for this result is that the C330S mutation made C-350 more accessible or closer to neighbor C-350 residues. However, we favor the hypothesis that BMH preferentially forms intramolecular C-330–C-350 cross-links in wt particles, while blocking the intramolecular reaction in C330S particles permits the intermolecular reaction to occur. Similar to C330S, all of the MHR cysteine substitution mutants showed putative CA-CA dimers upon BMH treatment (Fig. 8). This could occur if mutations in the MHR affected C-350 or C330S so that each now could react with a neighbor molecule. However, assuming that the block to intermolecular cross-linking via residue 350 is due to an intramolecular C-330–C-350 reaction, it is not clear how MHR mutations would affect this interaction. An alternative hypothesis is that cysteines of amphipathic MHR helices (5) on neighbor capsid molecules are in close enough proximity to cross-link. We currently are testing these structural predictions in vitro.

ACKNOWLEDGMENTS

The first two authors contributed equally to this research.

We gratefully acknowledge the gift of Hy5001 and Hy3D6.4DP from Epitope, Inc.; Hy183 (clone H12-5C) was obtained through the AIDS Research and Reference Reagent Program, Division of AIDS, NIAID, from Bruce Chesebro. Expert assistance with experiments was provided by Brent Berwin, Mark Hansen, Marylene Mougel, Jenny Stegeman-Olsen, Chin-Tien Wang, Mike Yamauchi, and Yaquiang Zhang, and we appreciated helpful discussions with Dick Brennan, Russell Jones, David Kabat, Scott Landfear, David Peyton, Maria Shumacher, and Stephan Wilkens.

This work was supported in part by grant 02301-16-RG from the American Foundation for AIDS Research and by grant 2R01 CA47088-07A3 from the National Cancer Institute.

REFERENCES

1. **Aldovini, A., and R. A. Young.** 1990. Mutations of RNA and protein sequences involved in human immunodeficiency virus type 1 packaging result in production of noninfectious virus. J. Virol. **64:**1920–1926.
2. **Baehler, M., F. Benfenati, F. Valtorta, A. J. Czernik, and P. Greengard.** 1989. Characterization of synapsin I fragments produced by cysteine-specific cleavage: a study of their interactions with F-actin. J. Cell Biol. **108:**1841–1849.
3. **Bennet, R. P., T. D. Nelle, and J. W. Wills.** 1993. Functional chimeras of the Rous sarcoma virus and human immunodeficiency virus Gag proteins. J. Virol. **67:**6487–6498.
4. **Cann, A. J., and J. Karn.** 1989. Molecular biology of HIV-1: new insights into the virus life cycle. AIDS **3**(Suppl. 1)**:**S19–S34.
5. **Clish, C. B., D. H. Peyton, and E. Barklis.** 1996. Spectroscopic study of an HIV-1 capsid protein major homology region peptide analog. FEBS Lett. **378:**43–47.
6. **Craven, R. C., A. E. Leure-duPree, C. R. Erdie, C. B. Wilson, and J. W. Wills.** 1993. Necessity of the spacer peptide between CA and NC in the Rous sarcoma virus Gag protein. J. Virol. **67:**6246–6252.
7. **Craven, R. C., A. E. Leure-duPree, R. A. Weldon, Jr., and J. W. Willis.** 1995. Genetic analysis of the major homology region of the Rous sarcoma virus Gag protein. J. Virol. **69:**4213–4227.
8. **Facke, M., A. Janetzko, R. L. Shoeman, and H. Krausslich.** 1993. A large deletion in the matrix domain of the human immunodeficiency virus *gag* gene redirects virus particle assembly from the plasma membrane to the endoplasmic reticulum. J. Virol. **67:**4972–4980.
9. **Gelderblom, H. R., M. Ozel, and G. Pauli.** 1989. Morphogenesis and morphology of HIV structure function relations. Arch. Virol. **106:**1–13.
10. **Gheysen, D., E. Jacobs, F. de Foresta, C. Thiriart, M. Francotte, D. Thines, and M. De Wilde.** 1989. Assembly and release of HIV-1 precursor pr55^{gag} virus-like particles from recombinant baculovirus-infected insect cells. Cell **59:**103–112.
11. **Gorelick, R. J., S. M. Nigida, Jr., J. W. Bess, Jr., L. O. Arthur, L. E. Henderson, and A. Rein.** 1990. Noninfectious human immunodeficiency virus type 1 mutants deficient in genomic RNA. J. Virol. **64:**3207–3211.
12. **Gottlinger, H. G., T. Dorfman, J. G. Sodroski, and W. A. Haseltine.** 1991. Effect of mutations affecting the p6 *gag* protein on human immunodeficiency virus particle release. Proc. Natl. Acad. Sci. USA **88:**3195–3199.
13. **Graham, R. M., and A. van der Eb.** 1973. A new technique for the assay of infectivity of human adenovirus 5 DNA. Virology **52:**456–467.
14. **Haffar, O., J. Garrigues, B. Travis, P. Moran, J. Zarling, and S.-L. Hu.** 1990. Human immunodeficiency virus-like, nonreplicating *gag-env* particles assemble in a recombinant vaccinia virus expression system. J. Virol. **64:**2653–2659.
15. **Han, K., C. Richard, G. Zhang, and A. Delacourte.** 1986. Sequence homology analysis of proteins by chemical cleavages: using a mono and two dimensional sodium dodecyl sulfate-polyacrylamide gel electrophoresis. Int. J. Biochem. **18:**1073–1082.
16. **Hansen, M., L. Jelinek, R. S. Jones, J. Stegeman-Olsen, and E. Barklis.** 1993. Assembly and composition of intracellular particles formed by Moloney murine leukemia virus. J. Virol. **67:**5163–5174.
17. **Hansen, M., L. Jelinek, S. Whiting, and E. Barklis.** 1990. Transport and

assembly of Gag proteins into Moloney murine leukemia virus. J. Virol. **64:**5306–5316.
18. **Hansen, M. H., and E. Barklis.** 1995. Structural interactions between retroviral Gag proteins examined by cysteine cross-linking. J. Virol. **69:**1150–1159.
19. **Henderson, L. E., M. A. Bowers, R. C. Sowder II, S. A. Serabyn, D. G. Johnson, J. W. Bess, Jr., L. O. Arthur, D. K. Bryant, and C. Fenselau.** 1992. Gag proteins of the highly replicative MN strain of human immunodeficiency virus type 1: posttranslational modifications, proteolytic processings, and complete amino acid sequences. J. Virol. **66:**1856–1865.
20. **Henderson, L. E., T. D. Copeland, R. C. Sowder, A. M. Schultz, and S. Oroszlan.** 1988. Analysis of proteins and peptides purified from sucrose gradient branded HTLV-III, p. 135–147. *In* D. Bolognesi (ed.), Human retroviruses and AIDS: approaches to prevention and therapy. Alan R. Liss, Inc., New York.
21. **Jones, T. A., G. Blaug, M. Hansen, and E. Barklis.** 1990. Assembly of Gag–β-galactosidase proteins into retrovirus particles. J. Virol. **64:**2265–2279.
22. **Karacostas, V., K. Nagashima, M. Gonda, and B. Moss.** 1989. Human immunodeficiency virus-like particles produced by a vaccinia virus expression vector. Proc. Natl. Acad. Sci. USA **86:**8964–8967.
23. **Karanjia, S., and E. Barklis.** Unpublished results.
24. **Laemmli, U. K.** 1970. Cleavage of structural proteins during the assembly of the head of bacteriophage T4. Nature (London) **227:**680–685.
25. **Leis, J., D. Baltimore, J. B. Bishop, J. Coffin, E. Fleissner, S. P. Goff, S. Oroszlan, H. Robinson, A. M. Skalka, H. M. Temin, and V. Vogt.** 1988. Standardized and simplified nomenclature for proteins common to all retroviruses. J. Virol. **62:**1808–1809.
26. **Louwagie, J., F. E. McCutchan, M. Peeters, T. P. Brennan, E. Sanders-Buell, G. A. Eddy, G. van der Groen, K. Fransen, G. M. Gershy-Damet, R. Deleys, and D. S. Burke.** 1993. Phylogenetic analysis of gag genes from 70 international HIV-1 isolates provides evidence for multiple genotypes. AIDS **7:**769–780.
27. **Mammano, F., A. Ohagen, S. Hoglund, and H. G. Gottlinger.** 1994. Role of the major homology region of human immunodeficiency virus type 1 in virion morphogenesis. J. Virol. **68:**4927–4936.
28. **Maniatis, T., E. F. Fritsch, and J. Sambrook.** 1982. Molecular cloning: a laboratory manual. Cold Spring Harbor Laboratory, Cold Spring Harbor, N.Y.
29. **Mervis, R. J., N. Ahmad, E. P. Lillehoj, M. G. Raum, F. H. R. Salazar, H. W. Chan, and S. Venkatesan.** 1988. The *gag* gene products of human immunodeficiency virus type 1: alignment within the *gag* open reading frame, identification of posttranslational modifications, and evidence for alternative *gag* precursors. J. Virol. **62:**3993–4002.
30. **Page, K. A., N. R. Landau, and D. R. Littman.** 1990. Construction and use of a human immunodeficiency virus vector for analysis of virus infectivity. J. Virol. **64:**5270–5276.
31. **Pakula, A. A., and M. I. Simon.** 1992. Determination of transmembrane structure by disulfide cross-linking: the Escherichia coli Tar receptor. Proc. Natl. Acad. Sci. USA **89:**4144–4148.
32. **Ratner, L., W. Haseltine, R. Patarca, K. J. Livak, B. Starich, S. F. Josephs, E. R. Doran, J. A. Rafalski, E. A. Whitehorn, K. Baumeisterm, L. Ivanoff, S. R. Petteway, Jr., M. L. Pearson, J. A. Lautenberger, T. S. Papas, J. Ghrayeb, N. T. Chang, R. C. Gallo, and F. Wong-Staal.** 1985. Complete nucleotide sequences of the AIDS virus, HTLV-III. Nature (London) **313:**277–284.
33. **Rhee, S. S., and E. Hunter.** 1990. Structural role of the matrix protein of type D retroviruses in Gag polyprotein stability and capsid assembly. J. Virol. **64:**4383–4389.
34. **Shioda, T., and H. Shibuta.** 1992. Production of human immunodeficiency virus (HIV)-like particles from cells infected with recombinant vaccinia viruses carrying the *gag* gene of HIV. Virology **175:**139–148.
35. **Smith, A. J., M.-I. Cho, M.-L. Hammarskjold, and D. Rekosh.** 1990. Human immunodeficiency virus type 1 $Pr55^{gag}$ and $Pr160^{gag\text{-}pol}$ expressed from a simian virus 40 late replacement vector are efficiently processed and assembled into viruslike particles. J. Virol. **64:**2743–2750.
36. **Stewart, L., G. Shatz, and V. Vogt.** 1990. Properties of avian retrovirus particles deficient in viral protease. J. Virol. **64:**5076–5092.
37. **Strambio-de-Castillia, C., and E. Hunter.** 1992. Mutational analysis of the major homology region of Mason-Pfizer monkey virus by use of saturation mutagenesis. J. Virol. **66:**7021–7032.
38. **Von Poblotzki, A., R. Wagner, M. Niedrig, G. Wanner, H. Wolf, and S. Modrow.** 1993. Identification of a region in the $Pr55^{Gag}$ polyprotein essential for HIV-1 particle formation. Virology **193:**981–985.
39. **Wang, C., and E. Barklis.** 1993. Assembly, processing, and infectivity of human immunodeficiency virus type 1 *gag* mutants. J. Virol. **67:**4264–4273.
40. **Wang, C., Y. Zhang, J. McDermott, and E. Barklis.** 1993. Conditional infectivity of a human immunodeficiency virus matrix domain mutant. J. Virol. **67:**7067–7076.
41. **Wills, J. W., and R. C. Craven.** 1991. Form, function and use of retroviral Gag proteins. AIDS **5:**639–654.
42. **Yu, X., Q. Yu, T. Lee, and M. Essex.** 1992. The C terminus of human immunodeficiency virus type 1 matrix protein is involved in early steps of the virus life cycle. J. Virol. **66:**5667–5670.
43. **Yu, X., X. Yuan, Z. Matsuda, T. Lee, and M. Essex.** 1992. The matrix protein of HIV-1 is required for incorporation of viral envelope protein into mature virions. J. Virol. **66:**4966–4971.
44. **Zhang, Y., and E. Barklis.** 1995. Nucleocapsid protein effects on the specificity of retrovirus RNA encapsidation. J. Virol. **69:**5716–5722.